Pergamon

Ocean Engng, Vol. 24, No. 5, pp. 479–495, 1997

0029–8018/97 $17.00 + 0.00

S0029–8018(96)00025-X

NONLINEAR DYNAMICS OF A COUPLED SURGE-HEAVE SMALL-BODY OCEAN MOORING SYSTEM

Oded Gottlieb* and Solomon C. S. Yim†

*Faculty of Mechanical Engineering, Technion-Israel Institute of Technology, Haifa, Israel
†Department of Civil Engineering, Oregon State University, Corvallis, Oregon, U.S.A.

(*Received* 15 *October* 1995; *accepted in final form* 25 *March* 1996)

Abstract—An investigation of coupled surge-heave motion of a symmetric small-body ocean mooring system is carried out in this paper. The dynamical system, formulated using a Lagrangian approach in the vertical plane of motion, is characterized by a strong geometric mooring nonlinearity and includes a quadratic relative motion Morison form for the hydrodynamic damping. Numerical simulations reveal complex periodic and aperiodic solutions which include torus multiplying and chaotic motion. The onset of instabilities is discussed and a comparison with a limiting decoupled surge model is performed.

1. INTRODUCTION

Complex nonlinear and chaotic responses have been reported extensively in the last decade for various numerical and approximate semi-analytical models of single and multiple-degree-of-freedom compliant offshore structures and mooring systems (e.g. Thompson, 1983; Papoulias and Bernitsas, 1988; Sharma *et al.*, 1988; Bishop and Virgin, 1988; Jiang and Schellin, 1990; Choi and Lou, 1991; Gottlieb and Yim, 1992 and Bernitsas and Garza-Rios, 1995). Subharmonic (Thompson *et al.*, 1984; Fujino and Sagara, 1990) and chaotic (Isaacson and Phadke, 1994) responses have also been shown in limited laboratory studies. Ocean mooring systems are characterized by a nonlinear mooring restoring force and a coupled hydrodynamic exciting force. The restoring force, which includes material discontinuities and geometric nonlinearities, has a unique equilibrium position, hence has a single well potential. The exciting force includes a quadratic fluid structure interaction viscous drag and harmonic wave induced inertial components. The drag component includes a bias, a quadratic nonlinearity and combined parametric and external excitation. The inertial component consists of biased external excitation which, for certain structural configurations, is complemented by an additional coupled nonlinear convective parametric excitation. Coupling of degrees of freedom further complicates system behavior.

Numerical and analytical investigations of systems which exhibit similar nonlinear properties have revealed complex behavior including coexisting periodic (harmonic, subharmonic, ultraharmonic, ultrasubharmonic) and aperiodic (quasiperiodic, chaotic) solutions defined by different initial conditions (Moon, 1992). System stability is governed by complex near resonant phenomena and sensitivity to initial conditions. While weakly nonlinear systems have been studied extensively from both classical (Nayfeh and Mook, 1979) and modern approaches (Guckenheimer and Holmes, 1986; Wiggins, 1990), analyses of complex single equilibrium point systems with a strong nonlinearity (which is a characteristic of ocean mooring systems) performed to date have been limited in their scope. Coupling of the degrees of freedom further complicates system analysis of finite multi-degree-of-freedom systems. Classical asymptotic techniques complemented by numerical analysis identify an enlarged bifurcation set and aperiodic solutions induced by internal resonance mechanisms in quadratically and cubical coupled oscillators (e.g. Miles, 1984a; Miles, 1984b; Nayfeh, 1988; Bajaj and Tousi, 1990; Cheng, 1991).

Ocean mooring systems include single and multi-point configurations (Skop, 1988) and are used to restrain the motion of compliant offshore structures (Leonard and Young, 1985). Single-point moorings (ABS, 1975) are characterized by curvature, material and hydrodynamic load nonlinearities (Leonard, 1988), whereas multi-point or spread moorings (API, 1987) include an additional geometric nonlinearity associated with mooring line angles (Bernitsas and Chung, 1990; Gottlieb and Yim, 1992). The mooring restoring force is formulated by incorporating these nonlinearities by exact or approximate formulation based on the mooring line characteristics and its orientation in the system. The nonlinear elastic force of a single cable line has been formulated by various methods. Examples include a quasi-static formulation of semi-empirical relations for elastic rope, catenary equations for chain (Leonard, 1988), and finite elements for steel cable. An alternative formulation is to incorporate a measured restoring force or its approximation. Examples of approximations by elementary functions include a piece-wise linear formulation (de Kat and Wichers, 1991), an exponential function description (Virgin and Bishop, 1988) and a truncated power series described by a quartic polynomial (Fujino and Sagara, 1990). Another single-point configuration, modeling coupled tanker-mooring tower motion, consists of a bi-linear formulation (Thompson *et al.*, 1984) and a least square approximation of a discontinuous restoring force resulting in a biased Duffing equation (Choi and Lou, 1991). The geometric nonlinearity of multi-point systems has either been approximated from data (Bishop and Virgin, 1988) or has been incorporated exactly in various time domain numerical models (e.g. Ansari and Khan, 1986; Chen and Chou, 1986) and a semi-analytical symmetric four-point system (Gottlieb, 1991) or a quasi-static mooring model (Bernitsas and Garza-Rios, 1995).

The hydrodynamic excitation includes coupled nonlinear fluid-structure interaction viscous drag and inertial components and requires separate treatment for small versus large bodies (Sarpkaya and Isaacson, 1981). Small bodies (with respect to flow wavelength) or structures with slender elements, do not alter the incident flow (Chakrabarti, 1987), whereas large bodies do change the characteristics of the flow field in the vicinity of the body and require knowledge of the scattered and radiated potential in addition to the incident potential. Therefore, small body problems are solved directly due to the explicit form of the hydrodynamic excitation, and large body problems require approximation of the hydrodynamic forces or simultaneous solution of the field-body boundary value problem. Body mooring systems (e.g. semi-submersibles, articulated towers) are generally solved by a relative motion Morison formulation whereas large body systems (e.g. ships, floating production systems) are solved by approximate quasi-static maneuvering equations (Abkowitz, 1972) or by numerical simulation. Numerical time domain simulation has been the primary tool for solution of both large (Wichers, 1988) and small body configurations (Bishop and Virgin, 1988). Evidence of strong subharmonic response, period multiplying route to chaotic motion and quasiperiodic instabilities appear in numerical models of both large and small body ocean mooring models that are subjected to combined steady and fast motion (Virgin and Bishop, 1988; Gottlieb and Yim, 1992; Choi and Lou, 1993). While the numerical time domain simulations incorporate exact forms of the dissipative forces, approximate analytical models typically neglect second order forces. Examples of such forces and their influence on system dynamics are the relative motion quadratic drag nonlinearities (Gottlieb and Yim, 1993) and second order drift forces in slow motion large body problems or convective nonlinearities that appear in small body formulations (Manners, 1992; Gottlieb, 1992). Although these nonlinear solutions exist in a relatively narrow parameter space, their magnitude is greater than that of the coexisting harmonic response.

The development of deep water compliant offshore structures requires a comprehensive understanding of strongly nonlinear ocean systems designed for relatively large displacements. Existing mooring systems analyses are portrayed by complex numerical models incorporating both structural and hydrodynamic nonlinearities or by idealized numerical or semi-analytical models where the nonlinearities are approximated and are in part described by their linearized or quasi-static representation. Identification and control of system instabilities are not always attainable in the complex numerical models and require extensive parametric analysis, whereas the linearized models are limited by their restrictive assumptions and do not always reveal true system behavior. As noted above, the multi-point mooring systems exhibits a variety of both structural and hydrodynamical nonlinearities. Simplification of environmental conditions via equivalent linearization methods or quasi-static representation and approximations of structural nonlinearities may reveal only partial qualitative results and will not determine all the mechanisms governing system instabilities and sensitivity to initial conditions.

In this paper we employ a Lagrangian formulation to obtain the multi-degree-of-freedom geometric nonlinearity of a symmetric four point system with the generalized forces consisting of an exciting force in the vertical plane of motion. The exciting force selected is that of a small body relative motion Morison formulation where the quadratic drag nonlinearity is retained exactly. Numerical simulations of the dynamical system reveal complex periodic and aperiodic solutions which include torus multiplying and chaotic motion. The onset of instabilities is discussed and a comparison with a limiting decoupled surge model is performed.

2. SYSTEM MODEL

The multi-point mooring system considered (Fig. 1) is formulated as a three-degree-of-freedom (surge–heave–pitch), rigid body hydrodynamically damped and excited nonlinear oscillator. The equations of motion are derived (Gottlieb, 1991) based on equilibrium of geometric restoring forces and small body motion under small amplitude monochromatic wave and current excitation. The equations of motion take the following classical form of three coupled nonlinear second order differential equations:

$$\ddot{\mathbf{X}} + \mathbf{D}(\dot{\mathbf{X}}) + \mathbf{R}(\mathbf{X}) = \mathbf{F}(\mathbf{X}, \dot{\mathbf{X}}, \ddot{\mathbf{X}}, t) \tag{1}$$

where $\mathbf{R}(\mathbf{X})$ and $\mathbf{D}(\mathrm{d}\mathbf{X}/\mathrm{d}t)$ are the system restoring force and structural damping vectors and $\mathbf{F}(\mathbf{X}, \mathrm{d}\mathbf{X}/\mathrm{d}t, \mathrm{d}^2\mathbf{X}/\mathrm{d}t^2, t)$ is the time dependent exciting force vector. $\mathbf{X}=(X_1, X_3, X_5)^{\mathrm{T}}$ is the system displacement vector representing surge (X_1), heave (X_3), and pitch (X_5) motions. Note that $(\cdot)$ is differentiation with respect to time and that the position of the body centroid at its equilibrium position is the origin of the reference inertial frame. The

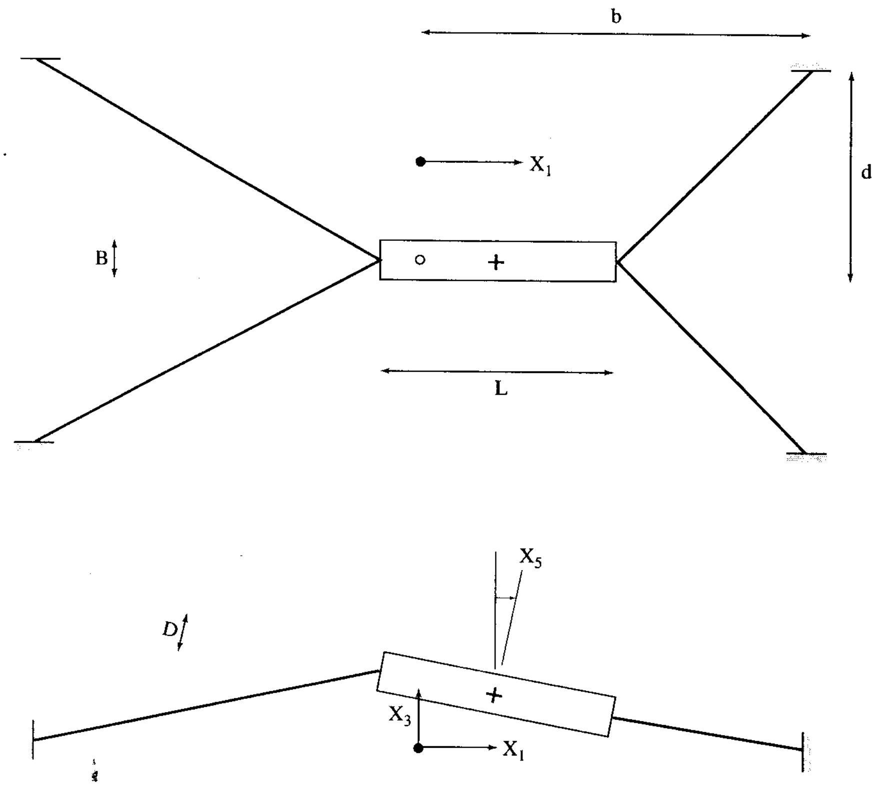

Fig. 1. Mooring assembly

exciting forces are formulated to account for nonlinear relative motions between the structure and the fluid whereas the restoring forces are formulated via a Lagrangian approach due to their complexity.

A symmetric multi-point mooring assembly (Fig. 1) yields an antisymmetric restoring force. Although the mooring lines may have linear elastic properties, the restoring force (stiffness) will include a strong geometric nonlinearity depending on the mooring angles. Two characteristic stiffness configurations which incorporate a material discontinuity are pretensioned and slack elastic cables. The discontinuity in the former case is due to loss of pretension in two lines whereas the latter case is based on an initial slackness. Both configurations can be described by a ratio (l_c/l_0) of initial mooring line length (l_c) to the length of the gap to be bridged by that line (l_0). Therefore, slack or pretensioned lines can be described by $l_c/l_0>1$ and $l_c/l_0<1$ respectively. The case of taut mooring lines represents the limits of both slack and pretensioned cables ($l_c=l_0$). In order to avoid modeling of the discontinuity by an infinite set of describing functions and to isolate the geometric nonlinearity, a continuous mooring restoring force ($\mathbf{R}_M$) is chosen. This force consists of both taut and pretensioned configurations ($l_c \leq l_0$) of linear elastic mooring lines which restrict the motion to the region where all lines retain their initial pretension. The stiffness nonlinearity can vary from a strongly nonlinear two-point system (b=0) to an almost linear four-point system ($b \gg d$ where b and d are the horizontal and vertical coordinates of the mooring point). The total restoring force ($\mathbf{R}$) includes the influence of mooring ($\mathbf{R}_M$) and hydrostatic buoyancy ($\mathbf{R}_B$).

The mooring restoring force [$\mathbf{R}_M(\mathbf{X})$] is conveniently derived from the potential function [$V_M(\mathbf{X})$] describing the pretensioned geometrical configuration of an axis-symmetric small body:

$$V_M(X_1, X_3, X_5) = K\{[l_1(X_1, X_3, X_5)-l_c]^2 + [l_2(X_1, X_3, X_5)-l_c]^2\} \quad (2)$$

where

$$l_{1,2} = [d^2 + \left(\frac{L}{2}\right)^2 + (b\pm X_1)^2 + X_3^2\pm LX_3 \sin X_5-L(b\pm X_1)\cos X_5]^{1/2} \quad (3)$$

and K is the elastic force coefficient, l_i (i=1, 2) is the *in situ* mooring line length and l_c is the initial pretensioned length of the mooring line. Note that the choice of the upper sign refers to l_1 and the lower sign to l_2.

Therefore, $\mathbf{R}_M(\mathbf{X})$=d$V_M(\mathbf{X})$/d$\mathbf{X}$ or:

$$R_{M1} = K\left\{4X_1 + l_c\left[(2b-L \cos X_5)\frac{l_1-l_2}{l_1l_2} -2X_1\frac{l_1+l_2}{l_1l_2}\right]\right\}$$

$$R_{M3} = K\left\{4X_3 + l_c\left[L \sin X_5\frac{l_1-l_2}{l_1l_2} -2X_3\frac{l_1+l_2}{l_1l_2}\right]\right\} \quad (4)$$

$$R_{M5} = K\left\{2bL\sin X_5 + l_c\left[L(X_1 \sin X_5 + X_3 \cos X_5)\frac{l_1-l_2}{l_1l_2} -bL \sin X_5\frac{l_1+l_2}{l_1l_2}\right]\right\}$$

The exciting force ($\mathbf{F}$) is formulated to account for the influence of both nonlinear drag ($\mathbf{F}_D$) and inertial effects ($\mathbf{F}_I$) exactly. The drag nonlinearity consists of a relative motion quadratic formulation whereas the inertial force consists of a temporal gradient.

$$F_{D1} = \frac{\rho}{2} C_{D1}A_{P1}(U_1-\dot{X}_1)\,|U_1-\dot{X}_1| \quad (5)$$

$$F_{D3} = \frac{\rho}{2} C_{D3}A_{P3}(U_3-\dot{X}_3)\,|U_3-\dot{X}_3|$$

$$F_{I1} = \rho V(1 + C_{A1})\frac{\partial U_1}{\partial t} -\rho VC_{A1}\ddot{X}_1 \quad (6)$$

$$F_{I3} = \rho V(1 + C_{A3})\frac{\partial U_3}{\partial t} -\rho VC_{A3}\ddot{X}_3$$

where

$$U_1 = U_0 + \omega a\frac{\cosh[k(X_3 + h)]}{\sinh(kh)}\cos(kX_1-\omega t) \quad (7)$$

$$U_3 = \omega a\frac{\sinh[k(X_3 + h)]}{\sinh(kh)}\sin(kX_1-\omega t)$$

and $C_{D1,3}$, $C_{A1,3}$ are hydrodynamic viscous drag and added mass coefficients; $A_{P1,3}$, V are projected drag areas and displaced volume; U_0 is a collinear current magnitude; a, ω, k are wave amplitude, cyclic frequency and wave number; ρ, g, h are water mass density, gravitational acceleration and water depth. Note that both projected drag areas ($A_{P1,3}$) and displaced volume (V) are frequency dependent functions when the body is surface piercing and that the projected areas are sensitive to the magnitude of body orientation (or pitch angle): $A_{P1}=B(D\cos X_5+L\sin X_5)$ and $A_{P3}=B(D\sin X_5+L\cos X_5)$. Furthermore, the relationship between wave frequency and number is determined by the linear dispersion equation: $\omega^2=gk\tanh(kh)$.

The drag and inertial components for pitch (F_{D5}, F_{M5}) can be formulated by integrating the differential moments ($\mathrm{d}M_{D,I}$) along the length (z': $-L/2$ to $+L/2$) of the body: $F_{D5}=\int \mathrm{d}M_D(z')$ and $F_{I5}=\int \mathrm{d}M_I(z')$ where:

$$\mathrm{d}M_{D5} = \frac{\rho}{2} BC_{D5}z'(U^* - z'\dot{X}_5) \mid U^* - z'\dot{X}_5 \mid \mathrm{d}z' \tag{8}$$

$$\mathrm{d}M_{I5} = \rho\forall\left\{(1 + C_{A5})\frac{\partial U^*}{\partial t} - C_{A5}z'\ddot{X}_5\right\}\mathrm{d}z'$$

and $U^*=U_{1S}\sin X_5+U_3\cos X_5$.

The structural damping force (**D**) consists of independent linearized friction components: $D_i=C_i\mathrm{d}X_i/\mathrm{d}t$ (i=1, 3, 5), where the damping coefficients are $C_{1,3,5}$.

The equations of motion are derived by the Lagrange approach:

$$\frac{\mathrm{d}}{\mathrm{d}t}\left(\frac{\partial \mathcal{L}}{\partial \dot{q}_i}\right) - \frac{\partial \mathcal{L}}{\partial q_i} = Q_i' \tag{9}$$

where $\mathcal{L}=T-V$ is the Lagrangian function and T, V are the kinetic and potential energies. q_i are generalized coordinates and Q_i' are generalized forces not derivable from the total potential. The displacement vector components are generalized coordinates and exciting force vector components are generalized forces as they are time dependent. The Lagrangian function is obtained from the kinetic and total potential energies. The potential consists of a mooring component (V_M in Equation (2)) and a body force due to hydrostatic buoyancy and gravity $[V_B=(\rho g\forall - Mg)X_3)]$.

$$T = \frac{M}{2}(\dot{X}_1^2 + \dot{X}_3^2) + \frac{I}{2}\dot{X}_5^2 \tag{10}$$

$$V = K\sum_i [l_i(X_1, X_3, X_5) - l_c]^2 + (\rho g\forall - Mg)X_3$$

where M, I are the body mass and moment of inertia and l_i (i=1, 2), the mooring line lengths are given in (Equation (3)).

Rearranging and scaling ($\mathbf{x}=\mathbf{X}/d$, $\theta=\omega t$) the equations of motion yields the following autonomous system which consists of seven coupled nonlinear first order ordinary differential equations:

$$\begin{aligned}\dot{\mathbf{x}} &= \mathbf{y}\\ \dot{\mathbf{y}} &= -\mathbf{R}(\mathbf{x}) - \mathbf{D}(\mathbf{y}) + \mathbf{F_D}(\mathbf{x}, \mathbf{y}, \theta) + \mathbf{F_I}(x, y, \theta)\\ \dot{\theta} &= \omega\end{aligned} \tag{11}$$

where $\mathbf{x}=(x_1, x_3, x_5)^T$, $\mathbf{y}=(y_1, y_3, y_5)^T$ are the length scaled system displacement and velocity vectors. Note that the velocity vector retains the time dimension.

For negligible pitch angles the system simplifies to the following:

$$\begin{aligned}
\dot{x}_1 &= y_1 \\
\dot{y}_1 &= -R_1(x_1, x_3) - \gamma_1 y_1 + F_{D1}(x_1, x_3, y_1, \theta) + F_{I1}(x_1, x_3, y_1, y_3, \theta) \\
\dot{x}_3 &= y_3 \\
\dot{y}_3 &= -R_3(x_1, x_3) - \gamma_3 y_3 + F_{D3}(x_1, x_3, y_1, \theta) + F_{I3}(x_1, x_3, y_1, y_3, \theta) \\
\dot{\theta} &= w
\end{aligned} \tag{12}$$

where

$$R_1 = \alpha\left[x_1 - \tau\left(\frac{l_1 + l_2}{l_1 l_2} x_1 - \beta \frac{l_1 - l_2}{l_1 l_2}\right)\right] \tag{13}$$

$$R_3 = \alpha\left[(1 + \sigma)x_3 - \tau\left(\frac{l_1 + l_2}{l_1 l_2} x_3\right)\right]$$

$$l_{1,2} = [1 + (\beta \pm x_1)^2 + x_3^2]^{1/2} \tag{14}$$

$$F_{D1} = \mu_1 \delta_1 \left(u_1 - \frac{y_1}{\omega}\right) |u_1 - \frac{y_1}{\omega}| \tag{15}$$

$$F_{D3} = \mu_3 \delta_3 \left(u_3 - \frac{y_3}{\omega}\right) |u_3 - \frac{y_3}{\omega}|$$

$$F_{I1} = \mu_1 \omega^2 \frac{\partial u_1}{\partial \theta}, \; F_{I3} = \mu_3 \omega^2 \frac{\partial u_3}{\partial \theta} \tag{16}$$

$$u_1 = f_0 + \frac{\chi}{\kappa} \frac{\cosh[\kappa(x_3 + h')]}{\sinh(\kappa h')} \cos(\kappa x_1 - \theta) \tag{17}$$

$$u_3 = \frac{\chi}{\kappa} \frac{\sinh[\kappa(x_3 + h')]}{\sinh(\kappa h')} \sin(\kappa x_1 - \theta)$$

and

$$\alpha_{1,3} = \frac{4K}{M + \rho V C_{A1,3}}, \; \beta = \frac{2b - L}{2d}, \; \tau = \frac{l_c}{2d}, \; \gamma_{1,3} = \frac{C_{1,3}}{M + \rho V C_{A1,3}},$$

$$\delta_{1,3} = \frac{A_{P1,3}}{2V} \frac{C_{D1,3}}{1 + C_{A1,3}} g\kappa \tanh(\kappa h'), \; \mu_{1,3} = \frac{\rho V(1 + C_{A1,3})}{M + \rho V C_{A1,3}}, \tag{18}$$

$$\sigma = \frac{g}{4K}(\rho V - M), \; f_0 = \frac{U_0}{\omega d}, \; \chi = ka, \; \kappa = kd, \; h' = \frac{h}{d}$$

Note that β, τ, σ, μ, κ, χ are nondimensional parameters whereas α, γ, δ and ω incorporate a time dimension. The restoring force is characterized by four parameters: α is a scaling amplitude, β describes the geometric nonlinearity in the horizontal plane, τ is a measure of the pretension in the mooring lines and $\sigma \geq 1$ characterizes non-negative buoyancy. The inertial exciting force is characterized by the wave frequency ω, a limiting wave steepness parameter $\chi < \pi/7$ and $\mu_1 > 1$ defines positive buoyancy. The damping force includes hydrodynamic drag δ and structural damping γ.

The system (12) nonlinearities appear in each of the principal equations ($d\mathbf{y}/dt$) in both the symmetric restoring (13) and drag (15) forces. Note that for a neutrally buoyant (σ=0) and strongly nonlinear configuration (β=0), the coupling between surge (x_1) and heave (x_3) is reduced to an identical hardening form for the geometric nonlinearity. The degree of nonlinearity is controlled by the geometric parameter β (Gottlieb and Yim, 1992).

3. THE UNMODULATED SYSTEM RESPONSE

The system (Equation (11)) does not have any fixed points in seven-dimensional space ($\mathbf{x}$, $\mathbf{y}$, θ) because $d\theta/dt=\omega$. However, a unique equilibrium position $[(\mathbf{x}, \mathbf{y})_e=\mathbf{0}]$ in six-dimensional space ($\mathbf{x}$, $\mathbf{y}$) can be determined via the associated integrable Hamiltonian system which yields an elliptic phase space described by the invariant Hamiltonian energy depicted (in any choice of two dimensions) by stable centers.

$$H(x_1, x_3, x_5, y_1, y_3, y_5) = \frac{1}{2}(y_1^2 + y_3^2 + y_5^2) + V(x_1, x_3, x_5) \tag{19}$$

Investigation of the structurally damped $[\boldsymbol{\gamma}\neq\mathbf{0}, \boldsymbol{\gamma}=(\gamma_1, \gamma_3)^T]$ unforced system ($F_{D1,3}=F_{I1,3}=0$) by local stability analysis is performed by linearizing the system about the unique equilibrium position (fixed point) at the origin $[(\mathbf{x}, \mathbf{y})_e=\mathbf{0}]$. The associated linearized system [or vector field: $d\mathbf{z}/dt=\mathbf{Az}$ where $\mathbf{z}=(\mathbf{x}-\mathbf{x}_e, \mathbf{y}-\mathbf{y}_e)$ and $\mathbf{A}$ is the derivative matrix of $-\mathbf{R}(\mathbf{x}) - \boldsymbol{\gamma}\mathbf{y}$ from (12) evaluated at $(\mathbf{x}, \mathbf{y})_e$] is structurally (asymptotically) stable if all the eigenvalues of the describing matrix ($\mathbf{A}$) have negative real parts. Consequently, the equilibrium solution $(\mathbf{x}, \mathbf{y})=(\mathbf{x}, \mathbf{y})_e$ of the nonlinear vector field is asymptotically stable. The following characteristic equation describes linearized vector field of the system ($\boldsymbol{\gamma} \neq \mathbf{0}$, $F_{D1,3}=F_{I1,3}=0$) about the fixed point $[(x_1, x_3, y_1, y_3)_e=\mathbf{0}]$:

$$\lambda^4 + a_3\lambda^3 + a_2\lambda^2 + a_1\lambda + a_0 = 0 \tag{20}$$

where

$$\begin{aligned} a_3 &= \gamma_1 + \gamma_3 \\ a_2 &= \gamma_1\gamma_3 + \alpha\left[2 + \sigma - 2\tau\frac{2 + \beta^2}{(1 + \beta^2)^{3/2}}\right] \\ a_1 &= \alpha\left[(1 + \sigma)\gamma_1 + \gamma_3 - 2\tau\frac{(1 + \beta^2)\gamma_1 + \gamma_3}{(1 + \beta^2)^{3/2}}\right] \\ a_0 &= \alpha^2\left[1 + \sigma - \frac{2\tau(2 + \beta^2)}{(1 + \beta^2)^{3/2}} + \left(\frac{2\tau}{1 + \beta^2}\right)^2\right] \end{aligned} \tag{21}$$

According to the Routh-Hurwitz criterion, the linear vector field near the origin is structurally stable [λ_i (i=1,...,4) have negative real parts] if and only if the coefficients a_i (i=0,...,4) and the following determinants ($D_{1,2}$) are always positive:

$$D_1 = a_2a_3 - a_1,\ D_2 = a_3(a_1a_2 - a_0a_3) - a_1^2 \tag{22}$$

Evaluation of the determinants results in the following:

$$D_1 = (\gamma_1 + \gamma_3)\gamma_1\gamma_3 + \alpha[\gamma_1 + (1+\sigma)\gamma_3] - 2\alpha\tau\frac{\gamma_1 + (1+\beta^2)\gamma_3}{(1+\beta^2)^{3/2}}$$

$$D_2 = \alpha(\gamma_1 + \gamma_3)\gamma_1\gamma_3\left\{[(1+\sigma)\gamma_1 + \gamma_3] - 2\tau\frac{(1+\beta^2)^2\gamma_1 + \gamma_3}{(1+\beta^2)^{3/2}}\right\} \tag{23}$$

$$+ \alpha^2(\gamma_1^2 + \gamma_3^2)\left\{1 + \sigma - 2\tau\frac{2+\sigma+\beta^2}{(1+\beta^2)^{3/2}} + \left(\frac{2\tau}{1+\beta^2}\right)^2\right\}$$

$$+ \alpha^2\gamma_1\gamma_3\left\{[1 + (1+\sigma)^2] - 2\tau\frac{1+\sigma+\sigma\beta^2+\beta^2}{(1+\beta^2)^{3/2}} + (2\tau)^2\frac{1+(1+\beta^2)^2}{(1+\beta^2)^3}\right\}$$

Investigation of the coefficients and determinants is done by introducing the pretension constraint $2\tau \le \sqrt{(1+\beta^2)}$ (i.e. $l_c \le l_0$). The resulting inequalities show that the vector field is structurally stable throughout parameter space (α, β, τ, σ, $\gamma_{1,3}$) with the exception of a neutrally buoyant (σ=0), taut (τ=1/2) right angle mooring configuration (β=0) which reveals a higher order degeneracy.

4. THE MODULATED SYSTEM RESPONSE

Perturbation of the nonlinear structurally stable unmodulated system by small amplitude wave excitation (17) for small values of structural and hydrodynamic damping enables formulation of the dynamical system as a weakly coupled two-degree-of-freedom dynamical system with quadratic and cubic nonlinearities due to the nonlinear drag and restoring force respectively:

$$\ddot{x}_1 + \omega_1^2 x_1 = \epsilon[-\hat{\gamma}_1\dot{x}_1 - \hat{R}_1(x_1, x_3) + \hat{F}_1(x_1, x_3, \dot{x}_1, \dot{x}_3, t)] \tag{24}$$
$$\ddot{x}_3 + \omega_3^2 x_3 = \epsilon[-\hat{\gamma}_3\dot{x}_3 - \hat{R}_3(x_1, x_3) + \hat{F}_3(x_1, x_3, \dot{x}_1, \dot{x}_3, t)]$$

where

$$\omega_1^2 = \alpha_1[1 - 2\tau(1+\beta^2)^{-3/2}],\quad \omega_3^2 = \alpha_3[(1+\sigma) - 2\tau(1+\beta^2)^{-1/2}] \tag{25}$$

and $(\epsilon\hat{\gamma}_{1,3}) = \gamma_{1,3}$ [$\gamma_{1,3}$ in (18)], $(\epsilon\hat{F}_{1,3}) = (F_{D1,3} + F_{I1,3})$ [$F_{(D,I)(1,3)}$ in (15), (16)] and $\epsilon\ R_{1,3}$ is obtained from (13).

Simulation of (24) results in stable periodic limit cycle motion about the structurally stable fixed point. However, for a specific damping threshold, excitation of (24) near resonance ($\omega \approx \omega_1$ or $\omega \approx \omega_2$) when the two linear natural frequencies are in internal resonance ($m\omega_3 = n\omega_1$) (cf. $\omega \approx \omega_1 = \omega_3$ in Miles, 1984; $\omega \approx \omega_1 = \omega_3/2$ in Nayfeh, 1988; $\omega \approx \omega_1 = \omega_3/3$ in Bajaj and Tousi, 1990) results in an amplitude modulated quasiperiodic solution in the form of a 2-torus. Furthermore, for even lower damping, the 2-torus may undergo further bifurcation resulting in chaotic motion following its destruction.

While weakly nonlinear mechanical systems exhibit near resonance amplitude modulations for small excitation levels in a narrow region of parameter space, a large domain of instability is obtained in a system with strong nonlinearity (cf. Cheng, 1991). An example model of a strongly nonlinear system with quasiperiodic response is a coupled single point mooring of a tanker and articulated tower (Choi and Lou, 1993). Furthermore, note that periodic response in models incorporating quasi-static maneuvering equations (via a Hopf bifurcation cf. Bernitsas and Chung, 1990) correspond to quasiperiodic motion as the periodicity in the 'slow motion' corresponds to modulated response in the fast time scale.

In this section we describe results obtained from a numerical simulation of the limiting strongly nonlinear (β=0) mooring system (12) for a neutrally buoyant condition (σ=0) with weak forcing (χ=0.1−0.3) and small structural and hydrodynamic damping ($\gamma_{1,3}$=0.01, δ=0.05, 0.1). Figure 2 depicts a displacement projection of the physical surge–heave phase space ($x_3(x_1)$) where an ellipse describes steady state periodic motion (Fig. 2a) and complex quasiperiodic motion is shown for two sets of environmental conditions (Fig. 2b, c). The fundamental torus describing the quasiperiodic response (Fig. 2b, c) undergoes further bifurcations which consist of tori multiplying. We describe this aperiodic response via a phase plane projection ($y_1(x_1)$) and its Poincaré map [$Y_{1P}(X_{1P})$: sampled at each forcing period=$2\pi/\omega$] and power spectra. Note that while a Poincaré map of an ultrasubharmonic signal will be described by a finite set of points the map of a quasiperiodic response consists of an infinite set of points organized on an invariant geometric shape. Thus, the torus tripling (Fig. 3) and doubling (Fig. 4) are depicted by an infinite number of Poincaré points on a closed shape. The doubled torus (Fig. 4) undergoes further bifurcations and quadruples (Fig. 5).

We compare a characteristic Poincaré map obtained for both coupled surge-heave system (Fig. 6) to that obtained from a limiting single degree-of-freedom surge model (Gottlieb and Yim, 1992). Note that while both attractors coexist with periodic solutions, the strange attractor of the coupled model coexists with a quasiperiodic attractor and as such is found for a smaller set of initial conditions.

5. CLOSING REMARKS

The investigation of coupled surge-heave motion of a symmetric small-body ocean mooring system carried out in this study, revealed complex aperiodic response. The dynamical system, formulated using a Lagrangian approach in the vertical plane of motion, was characterized by a strong geometric mooring nonlinearity and included a quadratic relative motion Morison form for the hydrodynamic excitation. Numerical simulations resulted in periodic and aperiodic solutions which included torus multiplying and chaotic response. The onset of additional quasiperiodic bifurcations was discovered and a comparison of chaotic attractors of both single and two-degree-of-freedom systems was performed employing a limiting decoupled surge model.

The nonlinear mooring was found to be governed by the geometric and pretension parameters and similar to results for the surge model, the amount of system dissipation from both structural damping and hydrodynamic drag control the thresholds and widths of the stability domains in parameter space. Results indicate that while bifurcation thresholds in both models are controlled by the magnitude of system dissipation, the coupling of the surge and heave degrees-of-freedom enlarges the domains of instability in comparison to those uncovered in previous work for the surge model in the ultrasubharmonic domain.

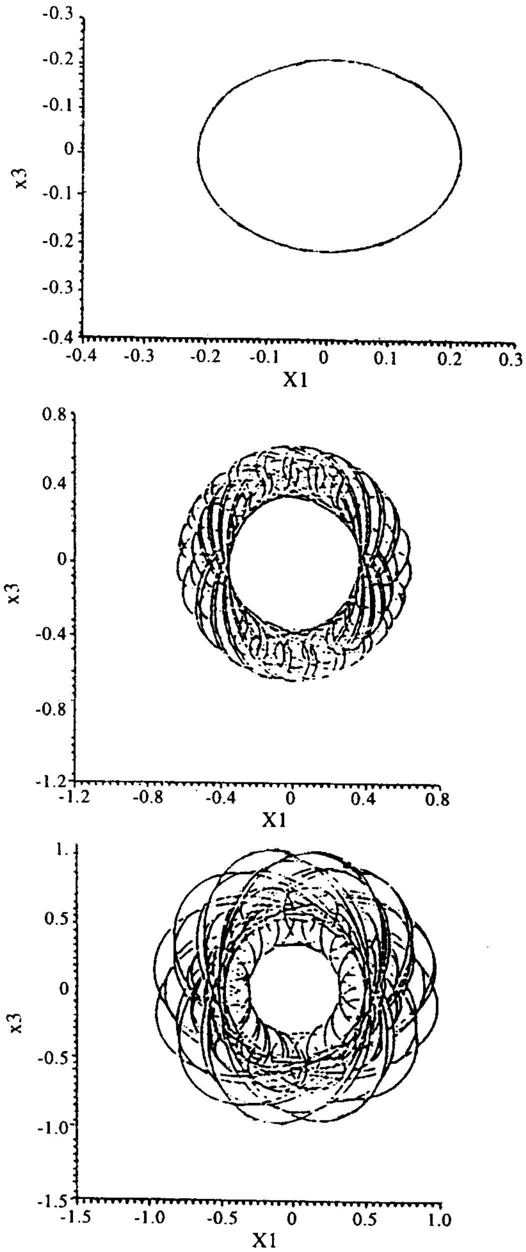

Fig. 2. Phase plane response (α=10, γ=0.01, δ=0.05); (a) periodic motion (ω=0.7, χ=0.1); (b) quasiperiodic motion (ω=1.01, χ=0.1); (c) quasiperiodic motion (ω=0.85, χ=0.3).

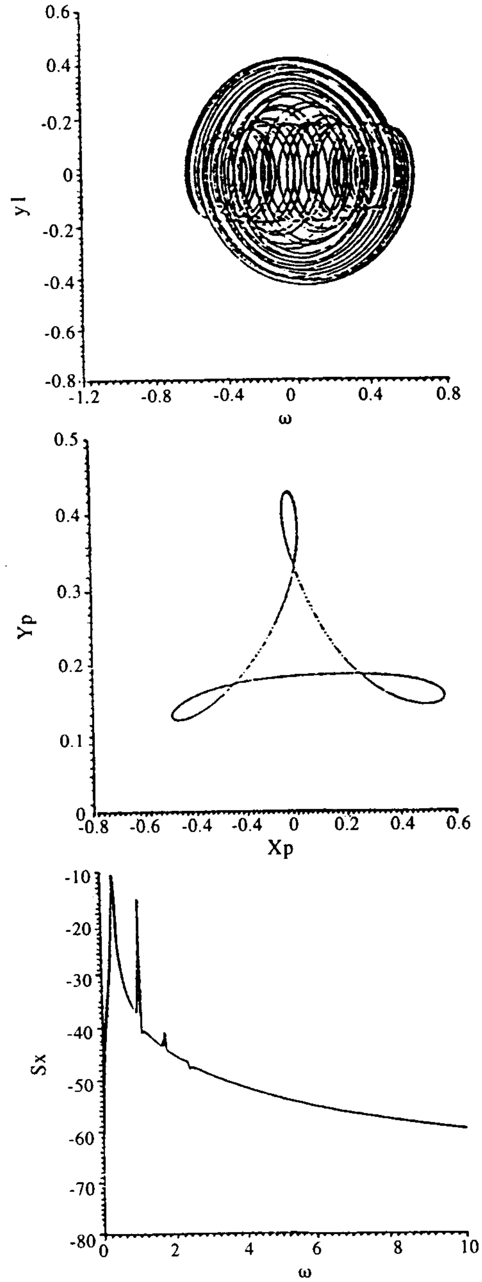

Fig. 3. Quasiperiodic torus tripling (α=1, γ=0.01, δ=0.1, ω=1.01, χ=0.1): (a) phase plane, (b) Poincaré map, (c) power spectra.

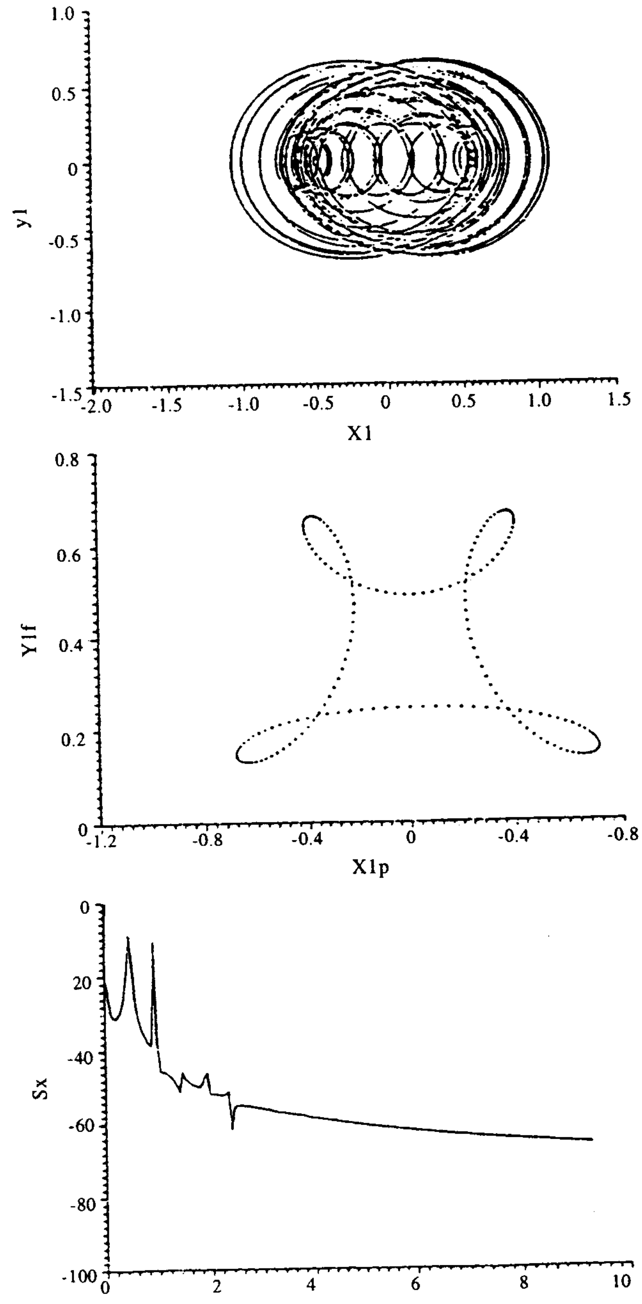

Fig. 4. Quasiperiodic torus doubling (α=10, γ=0.01, δ=0.1, ω=0.87, χ=0.2). (a) phase plane, (b) Poincaré map, (c) power spectra.

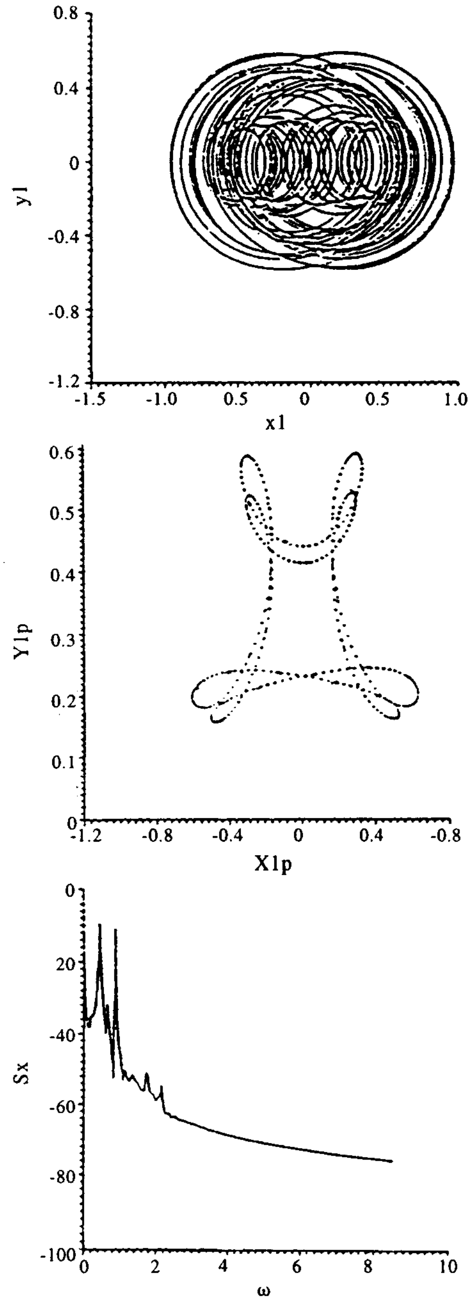

Fig. 5. Quasiperiodic torus quadrupling (α=10, γ=0.01, δ=0.1, ω=0.85, χ=0.3). (a) phase plane, (b) Poincaré map, (c) power spectra.

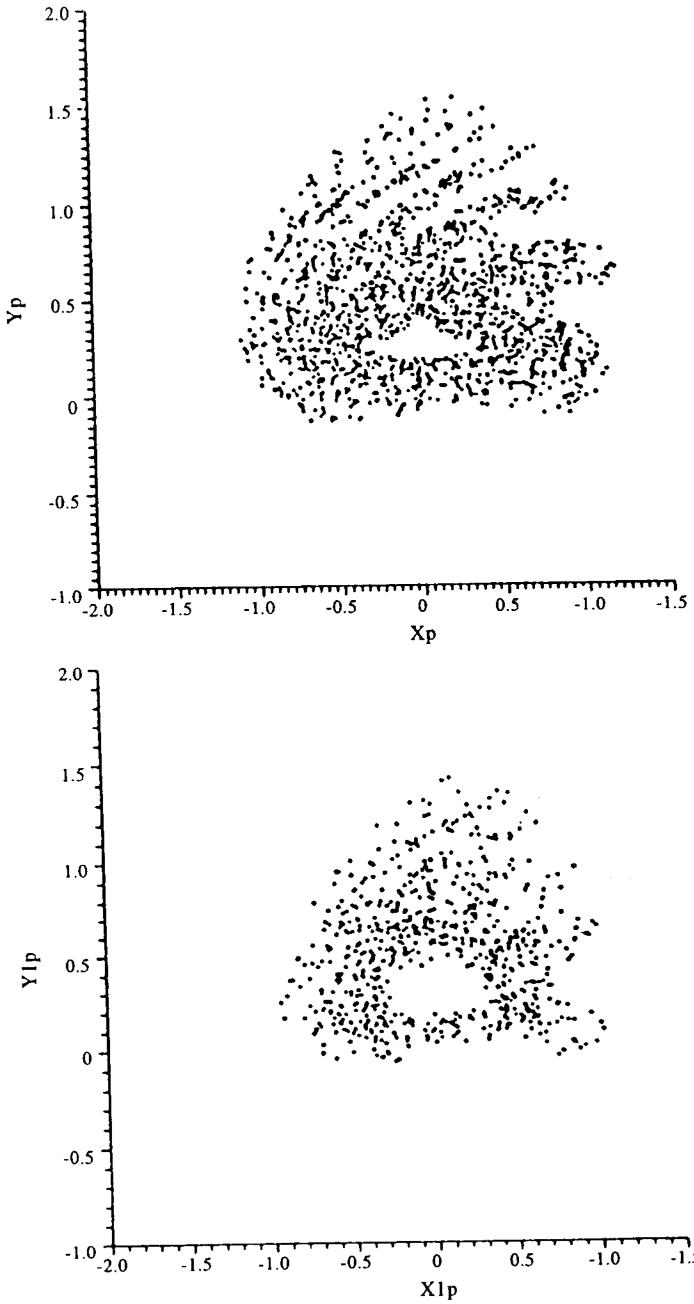

Fig. 6. Comparison of chaotic attractors (α=1, γ=0.01, δ=0.05, ω=0.81, χ=0.2): (a) single-degree-of-freedom system; (b) two-degree-of-freedom system.

Acknowledgements—This study was supported in part by the Office of Naval Research (Grant N00014-92-J-1221) and by the Fund for Promotion of Research at the Technion, Haifa, Israel.

REFERENCES

Abkowitz, M.A. 1972. *Stability and Motion Control of Ocean Vehicles*. MIT Press, Cambridge.

ABS. 1975. Single Point Mooring Systems—Rules for Building and Classing.

Ansari, K.A. and Khan, N.U. 1986. The effect of cable dynamics on the station-keeping response of a moored offshore vessel. *ASME Proc. 5 Int. Offshore Mech. Arctic Eng. Symp.* **3**, 514–521.

API. 1987. Analysis of spread mooring systems for floating drilling units.

Bajaj, A.K. and Tousi, S. 1990. Torus doubling and chaotic amplitude modulations in a two-degree-of-freedom resonantly forced mechanical system. *Int. J. Nonlinear Mech.* **25**, 625–641.

Bernitsas, M.M. and Chung, J.S. 1990. Nonlinear stability and simulation of two-line ship towing and mooring. *App. Ocean Res.* **11**, 153–166.

Bernitsas, M.M. and Garza-Rios, L.O. 1995. Effect of mooring line arrangement on the dynamics of spread mooring systems. *ASME Proc. Offshore Mech. Arctic Eng. Symp.* **1**, 237–252.

Bishop, S.R. and Virgin, L.N. 1988. The onset of chaotic motions of a moored semi-submersible. *ASME J. Offshore Mech. Arctic Eng.* **110**, 205–209.

Chakrabarti, S.K. 1987. *Hydrodynamics of Offshore Structures*, Springer-Verlag.

Chen, M.C. and Chou, F. 1986. Dynamic mooring system comparison for a deepwater semi-submersible. *ASME Proc, 5 Int. Offshore Mech. Arctic Eng. Symp.* **3**, 479–486.

Cheng, C. 1991. Invariant torus bifurcation series and evolution of chaos exhibited by a forced nonlinear vibration system. *Int. J. Nonlinear Mech.* **26**, 105–116.

Choi, H.S. and Lou, J.Y.K. 1991. Nonlinear behavior of an articulated loading platform. *App. Ocean Res.* **13**, 63–74.

Choi, H.S. and Lou, J.Y.K. 1993. Nonlinear mooring line induced slow drift motion of an alp-tanker. *Ocean Eng.* **20**, 233–246.

Fujino, M. and Sagara, N. 1990. An Analysis of Dynamic Behavior of an Articulated Column in Waves-Effects of Nonlinear Hydrodynamic Drag Force on the Occurrence of Subharmonic Oscillation. *J. Japan Society of Naval Architects*, 103–112 (in Japanese).

Gottlieb, O. 1991. Nonlinear oscillations, Bifurcations and chaos in ocean mooring systems, PhD. Thesis, Oregon State University.

Gottlieb, O. 1992. Bifurcations and routes to chaos in wave-structure interaction systems. *AIAA J. Guidance, Dynamics and Control* **15**, 832–839.

Gottlieb, O. and Yim, S.C.S. 1992. Nonlinear oscillations, bifurcations and chaos in a multi-point mooring systems with a geometric nonlinearity. *App. Ocean Res.* **14**, 291–297.

Gottlieb, O. and Yim, S.C.S. 1993. Drag induced instabilities in ocean mooring systems. *Ocean Eng.*

Guckenheimer, J. and Holmes, P. 1986. *Nonlinear Oscillations, Dynamical Systems and Bifurcation of Vector Fields*. Springer-Verlag, New York.

Isaacson, M. and Phadke, A. 1994. Chaotic motion of a nonlinearly moored structure. *Proc. 4th Int. Offshore and Polar Eng. Conf., Osaka, Japan* **3**, 338–345.

Jiang, T. and Schellin, T.E. 1990. Motion prediction of single-point moored tanker subjected to current, wind and waves. *ASME J. Offshore Mech. Arctic Eng.* **112**, 83–90.

De Kat, J.O. and Wichers, E.W. 1991. Behavior of a moored ship in unsteady current, wind and waves. *Marine Tech.* **28**, 251–264.

Leonard, J.W. and Young, R.A. 1985. Coupled response of compliant offshore platforms. *Eng. Struc.* **7**, 74–84.

Leonard, J.W. 1988. *Tension Structures, Behavior and Analysis*, McGraw-Hill, New York.

Manners, W. 1992. Hydrodynamic force on a moving circular cylinder submerged in a general fluid flow. *Proc. R. Soc. Lond.* **A438**, 331–339.

Miles, J.W. 1984a. Resonant motion of spherical pendulum. *Physica D.* **11**, 309–323.

Miles, J.W. 1984b. Resonantly forced motion of two quadratically coupled oscillators. *Physica D.* **13**, 247–260.

Moon, F.C. 1992. *Chaotic and Fractal Dynamics*. Wiley, New York.

Nayfeh, A.H. 1988. On the undesirable roll characteristics of ships in regular seas. *J. Ship Res.* **32**, 92–100.

Nayfeh, A.H. and Mook, D.T. 1979. *Nonlinear Oscillations*. Wiley, New York.

Papoulias, F.A. and Bernitsas, M.M. 1988. Autonomous oscillations, bifurcations and chaotic response of moored vessels. *J. Ship Res.* **32**, 220–228.

Sarpkaya, T. and Isaacson, M. 1981. *Mechanics of Wave Forces on Offshore Structures*. Van Nostrand Reinhold.

Sharma, S.D., Jiang, T. and Schellin, T.E. 1988. Dynamic instability and chaotic motions of a single-point moored tanker. *Proc. 17th ONR Symposium on Naval Hydrodynamics*. 543–563.

Skop, R.A. 1988. Mooring systems: a state of the art review. *ASME J. Offshore Mech. Arctic Eng.* **110**, 365–372.

Thompson, J.M.T. 1983. Complex dynamics of compliant offshore structures. *Proc. R. Soc. Lond.* **A387**, 407–427.

Thompson, J.M.T., Bokaian, A.R. and Ghaffari, R. 1984. Subharmonic and chaotic motions of compliant offshore structures and articulated mooring towers. *ASME J. Energy Resources Tech.* **106**, 191–198.

Virgin, L.N. and Bishop, S.R. 1988. Complex dynamics and chaotic responses in the time domain simulations of a floating structure. *Ocean Eng.* **15**, 71–90.

Wichers, J.E.W. 1988. A simulation model for a single point moored tanker. Maritime Res. Inst. Netherlands, Report no. 797.

Wiggins, S. 1990. *Introduction to Applied Nonlinear Dynamical Systems and Chaos*. Springer-Verlag, New York.